

## Relay Selection in the DF Relaying M2M Cooperative Networks

Lingwei Xu<sup>1</sup>, Hao Zhang<sup>2,3</sup> and T. Aaron Gulliver<sup>3</sup>

<sup>1</sup>*College of Information Science and Technology, Qingdao University of Science & Technology, Qingdao 266061, China*

<sup>2</sup>*College of Information Science and Engineering, Ocean University of China, Qingdao 266100, China*

<sup>3</sup>*Department of Electrical and Computer Engineering, University of Victoria, Victoria V8W 2Y2, Canada*

*gaomilaojia2009@163.com; zhanghao@ouc.edu.cn; agullive@ece.uvic.ca*

### Abstract

*The outage probability (OP) and average symbol error probability (ASEP) performance of multiple-mobile-relay-based mobile-to-mobile (M2M) networks with decode-and-forward (DF) relaying over  $N$ -Nakagami fading channels is investigated in this paper. The power allocation problem is formulated to determine how the overall transmit power should be shared between broadcasting and relaying phases for performance optimization. Then the OP and ASEP performance under different conditions is evaluated through numerical simulations to verify the analysis. The simulation results show that the fading coefficient, the number of cascaded components, the relative geometrical gain, the power-allocation parameter, and the number of mobile relays have an important influence on the OP and ASEP performance.*

**Keywords:** *M2M communication,  $N$ -Nakagami fading channels, decode-and-forward, outage probability, average symbol error probability, power allocation, relay selection*

## 1. Introduction

In recent years, mobile application development is swiftly expanding because users prefer to continue their social, entertainment, and business activities while on the go. The demand for higher capacity in mobile communication systems is motivated by the presence of service hot-spots and the widespread of content-rich web-based applications. Mobile-to-mobile (M2M) communication has attracted wide research interest from both academic and industrial fields. It is widely employed in many popular mobile wireless communication networks, such as inter-vehicular networks, intelligent highway networks and mobile ad-hoc networks [1]. However, the classical Rayleigh, Rician, or Nakagami fading channels have been found not to be applicable in M2M communication. When both the transmitter and receiver are in motion, the double-Rayleigh fading model has been found to be applicable [2]. The double-Nakagami fading model is adopted to provide a realistic description of the M2M channel in [3]. Using the Meijer's G-function, the  $N$ -Nakagami distribution is introduced and analyzed in [4].

Cooperative communication has emerged as a core component of future wireless networks since it provides high data rate communication over large geographical areas. It has been actively studied and considered in the standardization process of next-generation Broadband Wireless Access Networks (BWANs) such as Third Generation Partnership Project (3GPP) Long Term Evolution (LTE)-Advanced and IEEE 802.16m [5]. Using amplify-and-forward (AF) relaying scheme, pairwise error probability (PEP) of the cooperative inter-vehicular communication (IVC) system over double-Nakagami fading channels was investigated in [6]. In [7], by moment generating function (MGF) approach, the authors derived the lower bound on the exact average symbol error

probability (ASEP) expressions for AF relaying M2M networks over  $N$ -Nakagami fading channels. Exact average bit error probability (BEP) expressions for mobile-relay-based M2M cooperative networks with incremental decode-and-forward (IDF) relaying over  $N$ -Nakagami fading channels were derived in [8].

However, to the best knowledge of the author, the OP and ASEP performance of the DF relaying M2M networks with relay selection over  $N$ -Nakagami fading channels has not been investigated in the literature. In the present work, we extend our analysis for  $N$ -Nakagami case which subsumes double-Rayleigh in [2] and double-Nakagami in [3, 6] as special cases. The direct transmission between the source and destination is also considered. The main contributions are listed as follows:

1. Closed-form expressions are provided for the probability density function (PDF) and cumulative density functions (CDF) of the signal-to-noise ratio (SNR) over  $N$ -Nakagami fading channels. These are used to derive exact closed-form OP and ASEP expressions for DF relaying.
2. A power allocation minimization problem is formulated to determine the optimum transmit power distribution between the broadcasting and relaying phases.
3. The accuracy of the analytical results under different conditions is verified through numerical simulations. Results are presented which show that the fading coefficient, the number of cascaded components, the relative geometrical gain, and the power allocation parameter have a significant influence on the OP and ASEP performance.
4. The derived OP and ASEP expressions can be used to evaluate the OP and ASEP performance of the vehicular communications systems employed in inter-vehicular communications, intelligent highway applications and mobile ad-hoc applications.

The rest of the paper is organized as follows. The multiple-mobile-relay-based M2M system model with relay selection is presented in Section 2. Section 3 provides the exact closed-form OP expressions for DF relaying. The exact ASEP expressions are derived in Section 4. In Section 5, the OP is optimized based on the power allocation parameter. Section 6 conducts Monte Carlo simulations to verify the analytical results. Concluding remarks are given in Section 7.

## 2. The System Model

We consider a multi-mobile-node cooperation model, as depicted in Figure 1. It consists of a single mobile source (MS) node,  $L$  mobile relay (MR) nodes, and a single mobile destination (MD) node. The nodes operate in half-duplex mode, which are equipped with a single pair of transmitter and receiver antennas.

According to [6], we let  $d_{SD}$ ,  $d_{SR_l}$ , and  $d_{RD_l}$  represent the distances of the source to the destination (MS $\rightarrow$ MD), the source to the  $l$ th relay (MS $\rightarrow$ MR $_l$ ), and the  $l$ th relay to destination (MR $_l\rightarrow$ MD) links, respectively. The relative gain of the MS to MD link is  $G_{SD}=1$ , the relative gains of the MS to MR $_l$  and MR $_l$  to MD links are  $G_{SR_l}=(d_{SD}/d_{SR_l})^\nu$  and  $G_{RD_l}=(d_{SD}/d_{RD_l})^\nu$ , respectively, where  $\nu$  is the path loss coefficient [9]. The relative geometrical gain  $\mu_l = G_{SR_l}/G_{RD_l}$  (in decibels) indicates the location of the  $l$ th relay with respect to the source and destination. When the  $l$ th relay is close to the destination node, the values of  $\mu_l$  are negative. When the  $l$ th relay is close to the source node, the values of  $\mu_l$  are positive. When the  $l$ th relay has the same distance to the source and destination nodes,  $\mu_l$  is 0dB.

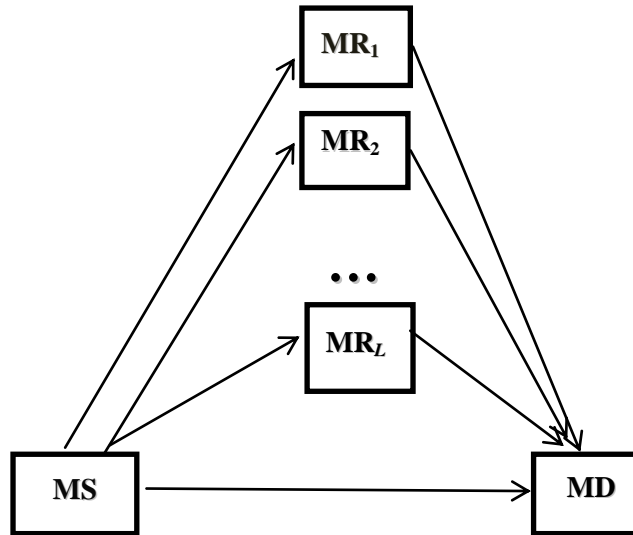


Figure 1. The System Model

Let  $h=h_k$ ,  $k \in \{SD, SRL, RDL\}$ , represent the complex channel coefficients of  $MS \rightarrow MD$ ,  $MS \rightarrow MR_l$ , and  $MR_l \rightarrow MD$  links, respectively. We assume that the links are subject to independently and identically distributed (i.n.i.d)  $N$ -Nakagami fading.  $h$  follows  $N$ -Nakagami distribution, which is given as [4]

$$h = \prod_{i=1}^N a_i \quad (1)$$

where  $N$  is the number of cascaded components,  $a_i$  is a Nakagami distributed random variable with PDF as

$$f(a) = \frac{2 m^m}{\Omega^m \Gamma(m)} a^{2m-1} \exp\left(-\frac{m}{\Omega} a^2\right) \quad (2)$$

where  $\Gamma(\cdot)$  is the Gamma function,  $m$  is the fading coefficient and  $\Omega$  is a scaling factor. The PDF of  $h$  is given by [4]

$$f(h) = \frac{2}{h \prod_{i=1}^N \Gamma(m_i)} G_{0,N}^{N,0} \left[ h^2 \prod_{i=1}^N \frac{m_i}{\Omega_i} \middle|_{m_1, \dots, m_N}^- \right] \quad (3)$$

where  $G[\cdot]$  is the Meijer's G-function.

Let  $y=|h_k|^2$ ,  $k \in \{SD, SRL, RDL\}$ , namely,  $y_{SD}=|h_{SD}|^2$ ,  $y_{SRL}=|h_{SRL}|^2$ , and  $y_{RDL}=|h_{RDL}|^2$ . The corresponding CDF and PDF of  $y$  can be derived as [4]

$$F(y) = \frac{1}{\prod_{i=1}^N \Gamma(m_i)} G_{1,N+1}^{N,1} \left[ y \prod_{i=1}^N \frac{m_i}{\Omega_i} \middle|_{m_1, \dots, m_N, 0}^+ \right] \quad (4)$$

$$f(y) = \frac{1}{y \prod_{i=1}^N \Gamma(m_i)} G_{0,N}^{N,0} \left[ y \prod_{i=1}^N \frac{m_i}{\Omega_i} \middle|_{m_1, \dots, m_N}^- \right] \quad (5)$$

Based on the DF cooperation protocol, the received signals  $r_{SD}$  and  $r_{SRL}$  at the MD and

MR<sub>*l*</sub> during the first time slot can be written as

$$r_{SD} = \sqrt{KE} h_{SD} x + n_{SD} \quad (6)$$

$$r_{SR_l} = \sqrt{G_{SR_l} KE} h_{SR_l} x + n_{SR_l} \quad (7)$$

where  $x$  denotes the transmitted signal,  $n_{SR_l}$  and  $n_{SD}$  are the zero-mean complex Gaussian random variables with variance  $N_0/2$  per dimension. Here,  $E$  is the total energy which is used by both source and relay terminals during two time slots.  $K$  is the power-allocation parameter that controls the fraction of power reserved for the broadcasting phase. If  $K=0.5$ , the equal power allocation (EPA) scheme is used.

During the second time slot, the MR<sub>*l*</sub> decodes its received signal. The received signal at the MD is therefore given by

$$r_{RD_l} = k \left( \sqrt{G_{RD_l}(1-K)E} h_{RD_l} x + n_{RD_l} \right) \quad (8)$$

Where  $k = 1$ , the signal is correctly decoded by MR<sub>*l*</sub>, otherwise  $k=0$ .  $n_{RD_l}$  is a conditionally zero-mean complex Gaussian random variable with variance  $N_0/2$  per dimension.

We define the decoding set  $C$  as the set of relays with the ability to fully decode the source message correctly. Based on the selection cooperation protocol, only the best relay is activated in each transmission session. In our scheme, the MD firstly chooses the best relay based on the following criterion

$$\gamma_{SR^*_D} = \mathop{\text{max}}_{i \in C} (\gamma_{RD_i}) \quad (9)$$

where

$$\gamma_{RD_i} = \frac{(1-K)G_{RD_i} |h_{RD_i}|^2 E}{N_0} = (1-K)G_{RD_i} |h_{RD_i}|^2 \bar{\gamma} \quad (10)$$

If selection combining (SC) method is used at MD, the output SNR can then be calculated as [10]

$$\gamma_{SC} = \mathop{\text{max}} (\gamma_{SD}, \gamma_{SR^*_D}) \quad (11)$$

where

$$\gamma_{SD} = \frac{K |h_{SD}|^2 E}{N_0} = K |h_{SD}|^2 \bar{\gamma} \quad (12)$$

Thus, we can obtain the CDF of the output SNR at MD as

$$F_{\gamma_{SC}}(r) = F_{\gamma_{SD}}(r) F_{\gamma_{SR^*_D}}(r) \quad (13)$$

and the PDF as

$$f_{\gamma_{SC}}(r) = f_{\gamma_{SD}}(r) F_{\gamma_{SR^*_D}}(r) + F_{\gamma_{SD}}(r) f_{\gamma_{SR^*_D}}(r) \quad (14)$$

The CDF of  $\gamma_{SD}$  can be given as

$$F_{\gamma_{SD}}(r) = \frac{1}{\prod_{i=1}^N \Gamma(m_i)} G_{1,N+1}^{N,1} \left[ \frac{r}{\gamma_{SD}} \prod_{i=1}^N \frac{m_i}{\Omega_i} \middle|_{m_1, \dots, m_N, 0} \right] \quad (15)$$

where

$$\overline{\gamma_{SD}} = K \overline{\gamma} \quad (16)$$

The corresponding PDF can be obtained as

$$f_{\gamma_{SD}}(r) = \frac{1}{r \prod_{i=1}^N \Gamma(m_i)} G_{0,N}^{N,0} \left[ \frac{r}{\gamma_{SD}} \prod_{i=1}^N \frac{m_i}{\Omega_i} \middle|_{m_1, \dots, m_N} \right] \quad (17)$$

### 3. The OP of DF Relaying M2M Networks

In this section, the exact closed-form OP expressions for the DF relaying M2M networks with relay selection are derived.

The mutual information between the MS and MR<sub>l</sub> is given as

$$I_{SRl} = \frac{1}{2} \log_2 (1 + \gamma_{SRl}) \quad (18)$$

where

$$\gamma_{SRl} = \frac{G_{SRl} K |h_{SRl}|^2 E}{N_0} = G_{SRl} K |h_{SRl}|^2 \overline{\gamma} \quad (19)$$

If the mutual information is lower than spectral efficiency  $R$ , the MR<sub>l</sub> will not be used for cooperation. It can be denoted as

$$\Pr(I_{SRl} < R) = \Pr\left(\frac{1}{2} \log_2 (1 + \gamma_{SRl}) < R\right) \quad (20)$$

Following the method in [2], we define a random variable  $\gamma_l$ , which represents the instantaneous SNR received at MD via MR<sub>l</sub>. The CDF of  $\gamma_l$  can be given as

$$\begin{aligned} F_{\gamma_l}(r) &= \Pr(I_{SRl} < R) + (1 - \Pr(I_{SRl} < R)) F_{\gamma_{RDl}}(r) \\ &= I_1 + I_2 \end{aligned} \quad (21)$$

From Appendix A, a new closed-form expression for the CDF of  $\gamma_l$  is given as

$$F_{\gamma_l}(r) = \left( \frac{1}{\prod_{j=1}^N \Gamma(m_j)} G_{1,N+1}^{N,1} \left[ \frac{r_{th}}{\gamma_{SRl}} \prod_{j=1}^N \frac{m_j}{\Omega_j} \right]_{m_1, \dots, m_N, 0} \right) + \left( 1 - \frac{1}{\prod_{j=1}^N \Gamma(m_j)} G_{1,N+1}^{N,1} \left[ \frac{r_{th}}{\gamma_{SRl}} \prod_{j=1}^N \frac{m_j}{\Omega_j} \right]_{m_1, \dots, m_N, 0} \right) \times \left( \frac{1}{\prod_{jj=1}^N \Gamma(m_{jj})} G_{1,N+1}^{N,1} \left[ \frac{r}{\gamma_{RDl}} \prod_{jj=1}^N \frac{m_{jj}}{\Omega_{jj}} \right]_{m_1, \dots, m_N, 0} \right) \quad (22)$$

The total SNR at MD given in (9) can be rewritten as

$$\gamma_{SR^*D} = \mathbf{max}_{1 \leq l \leq L} (\gamma_l) \quad (23)$$

The CDF can be given as

$$F_{\gamma_{SR^*D}}(r) = \prod_{l=1}^L F_{\gamma_l}(r) \quad (24)$$

The CDF of  $\gamma_{SC}$  can be given as

$$F_{\gamma_{SC}}(r) = F_{\gamma_{SD}}(r) F_{\gamma_{SR^*D}}(r) \quad (25)$$

The OP of the DF relaying M2M networks with relay selection can be expressed as

$$F_{\gamma_{SC}}(R_{th}) = \frac{1}{\prod_{i=1}^N \Gamma(m_i)} G_{1,N+1}^{N,1} \left[ \frac{R_{th}}{\gamma_{SD}} \prod_{i=1}^N \frac{m_i}{\Omega_i} \right]_{m_1, \dots, m_N, 0} \times \left( \frac{1}{\prod_{j=1}^N \Gamma(m_j)} G_{1,N+1}^{N,1} \left[ \frac{r_{th}}{\gamma_{SRl}} \prod_{j=1}^N \frac{m_j}{\Omega_j} \right]_{m_1, \dots, m_N, 0} \right) + \left( 1 - \frac{1}{\prod_{j=1}^N \Gamma(m_j)} G_{1,N+1}^{N,1} \left[ \frac{r_{th}}{\gamma_{SRl}} \prod_{j=1}^N \frac{m_j}{\Omega_j} \right]_{m_1, \dots, m_N, 0} \right) \times \left( \frac{1}{\prod_{jj=1}^N \Gamma(m_{jj})} G_{1,N+1}^{N,1} \left[ \frac{R_{th}}{\gamma_{RDl}} \prod_{jj=1}^N \frac{m_{jj}}{\Omega_{jj}} \right]_{m_1, \dots, m_N, 0} \right) \quad (26)$$

where  $R_{th}$  is the threshold for correct detection at MD.

#### 4. The ASEP of DF Relaying M2M Networks

The ASEP of the DF relaying M2M networks with relay selection is given as [11]

$$P = \frac{a\sqrt{b}}{2\sqrt{\pi}} \int_0^{\infty} \frac{\exp(-br)}{\sqrt{r}} F_{\gamma_{sc}}(r) dr \quad (27)$$

where  $a$  and  $b$  are the parameters determined by modulation type. For instance, for  $q$ -ary PAM modulation,  $a=2(q-1)/q$ ,  $b=3/(q^2-1)$ ; for  $q$ -ary PSK modulation,  $a=2$ ,  $b=\sin^2(\pi/q)$ .

Substituting (25) into (27), the exact expression for the ASEP is given as

$$P = \frac{a\sqrt{b}}{2\sqrt{\pi}} G \quad (28)$$

where

$$G = \int_0^{\infty} \frac{1}{\sqrt{r}} G_{0,1}^{1,0} \left[ br \left| - \right. \right] G_{1,N+1}^{N,1} \left[ \frac{r}{\gamma_{RDl}} \prod_{i=1}^N \frac{m_i}{\Omega_i} \Big|_{m_1, \dots, m_N, 0} \right] \times \left( \frac{1}{\prod_{j=1}^N \Gamma(m_j)} G_{1,N+1}^{N,1} \left[ \frac{r_{th}}{\gamma_{SRl}} \prod_{j=1}^N \frac{m_j}{\Omega_j} \Big|_{m_1, \dots, m_N, 0} \right] + \left( \prod_{l=1}^L \left[ 1 - \frac{1}{\prod_{j=1}^N \Gamma(m_j)} G_{1,N+1}^{N,1} \left[ \frac{r_{th}}{\gamma_{SRl}} \prod_{j=1}^N \frac{m_j}{\Omega_j} \Big|_{m_1, \dots, m_N, 0} \right] \right) \times \frac{1}{\prod_{jj=1}^N \Gamma(m_{jj})} G_{1,N+1}^{N,1} \left[ \frac{r}{\gamma_{RDl}} \prod_{jj=1}^N \frac{m_{jj}}{\Omega_{jj}} \Big|_{m_1, \dots, m_N, 0} \right] \right) dr \quad (29)$$

#### 5. Optimized Power Allocation

To further improve the performance, we aim to optimally allocate the power between broadcasting and relaying phases. For optimization of the power allocation, we consider the OP as our objective function. The resulting OP needs to be minimized with respect to the power-allocation parameter  $K$  ( $0 \leq K \leq 1$ ).

Figure 2 presents the effect of the power-allocation parameter  $K$  on the OP performance with various values of SNR. The number of cascaded components is  $N=2$ . The fading coefficient is  $m=2$ . The relative geometrical gain is  $\mu=0$ dB. The number of mobile relays is  $L=2$ . The given threshold is  $r_{th}=4$ dB. Simulation results show that the OP performance is improved with the SNR increased. For example, when  $K=0.6$ , the OP is  $1.6 \times 10^{-1}$  with SNR=10dB,  $6 \times 10^{-3}$  with SNR=20dB,  $6.8 \times 10^{-4}$  with SNR=30dB. When SNR=10dB, the optimum value of  $K$  is 0.65; SNR=15dB, the optimum value of  $K$  is 0.61; SNR=30dB, the optimum value of  $K$  is 0.59. This indicates that the equal power allocation (EPA) scheme is not the best scheme.

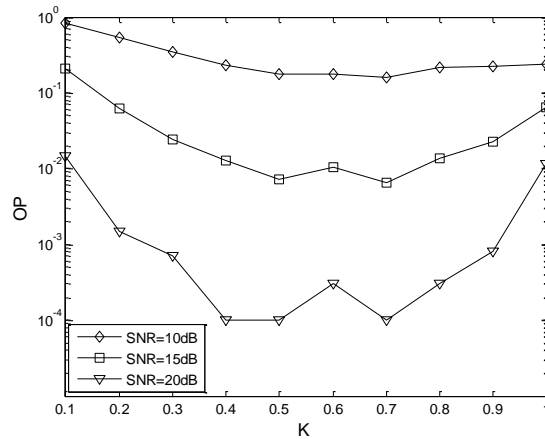


**Figure 2. The Effect of the Power-Allocation Parameter  $K$  on the OP Performance**

From Figure 2, it can readily be checked that these expressions are convex functions with respect to  $K$ . The convexity of the OP functions under consideration guarantees that the local minimum found through optimization will indeed be a global minimum. Unfortunately, an analytical solution for power allocation values in the general case is very difficult. We resort to numerical methods to solve this optimization problem. The optimum power allocation (OPA) values can be obtained a priori for given values of operating SNR and propagation parameters. The OPA values can be stored for use as a lookup table in practical implementation.

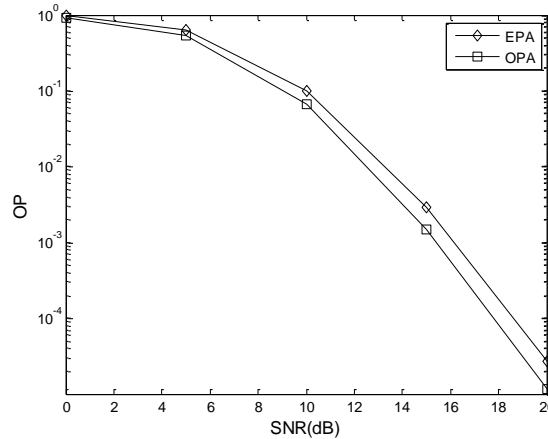
In Table 1, we present optimum values of  $K$  with various values of SNR. We assume that the number of cascaded components is  $N=2$ , the fading coefficient is  $m=2$ , the relative geometrical gain is  $\mu=-5$  dB, the number of mobile relays is  $L=2$ , and the given threshold is  $r_{th}=4$ dB. This indicates that when relay is close to destination, more than 70% of power should be used in broadcast phase.

**Table 1. OPA Parameters  $K$**

SNR	$K$
0	0.99
5	0.75
10	0.72
15	0.72
20	0.72

Figure 3 presents the effect of the EPA and OPA on the OP performance. For OPA, the values of  $K$  are used in Table 1. For EPA,  $K=0.5$ . These results show that the OP performance of OPA is better than that of EPA. For example, with SNR=15 dB, the OP is  $1.5 \times 10^{-3}$  for OPA, while  $3 \times 10^{-3}$  for EPA.

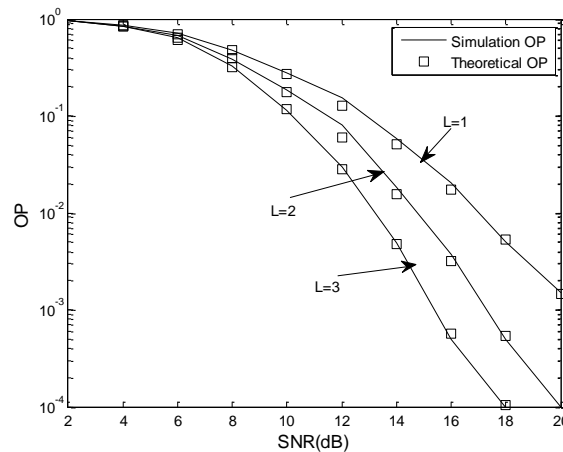




**Figure 3. The Effect of the EPA and OPA on the OP Performance**

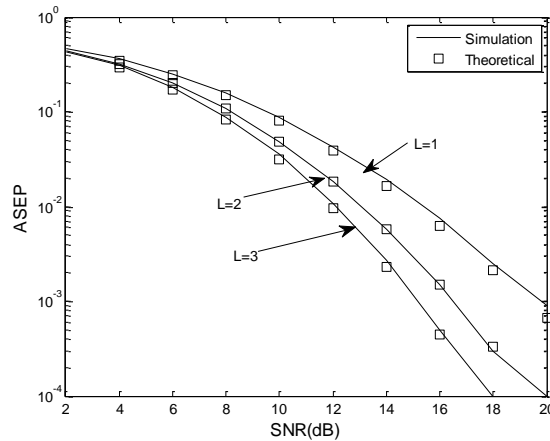
## 6. Numerical Results

In this section, we present Monte-Carlo simulations to confirm the derived analytical results. Additionally, random number simulation was done to confirm the validity of the analytical approach. All the computations were done in MATLAB and some of the integrals were verified through MAPLE. The total energy is  $E = 1$ . The fading coefficient is  $m=1, 2, 3$ , the number of cascaded components is  $N=2, 3, 4$ , the number of mobile relays is  $L=1, 2, 3$ , and the relative geometrical gain is  $\mu=15 \text{ dB}, 0 \text{ dB}, -15 \text{ dB}$ , respectively. For different values of  $m, N, \mu, L$ , the optimized values of  $K$  are different. In Figure 4, 5, 6, 7, 8, we only want to present the effect of  $m, N, \mu, L$  on the OP and ASEP, respectively, so the value of  $K$  should remain unchanged. Here, we choose  $K=0.5$ .



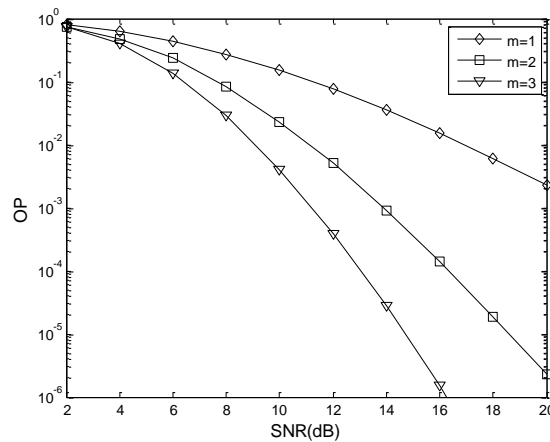
**Figure 4. The Effect of the Number of Mobile Relays  $L$  on the OP Performance**

Figure 4 presents the effect of the number of mobile relays  $L$  on the OP performance. The number of cascaded components is  $N=2$ . The fading coefficient is  $m=2$ . The power-allocation parameter is  $K=0.5$ . The relative geometrical gain is  $\mu=0 \text{ dB}$ . The given threshold is  $r_{th}=4 \text{ dB}$ . The number of mobile relays is  $L=1, 2, 3$ . Simulation results show that the OP performance is improved with the number of mobile relays  $L$  increased. For example, when  $\text{SNR}=12\text{dB}$ , the OP is  $1.3 \times 10^{-1}$  with  $L=1$ ,  $6 \times 10^{-2}$  with  $L=2$ ,  $2.8 \times 10^{-2}$  with  $L=3$ . In order to improve the OP performance,  $L$  should be increased. With  $L$  fixed, an increase in the SNR decreases the OP.



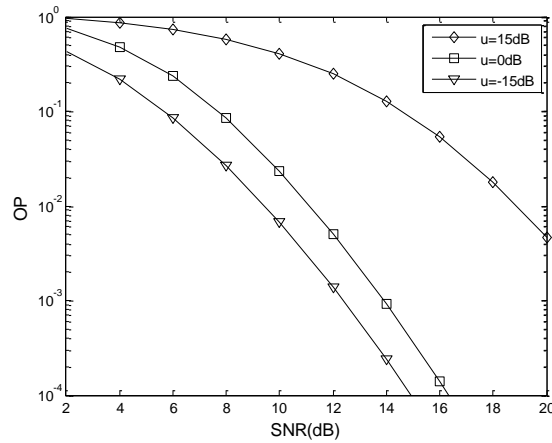
**Figure 5. The Effect of the Number of Mobile Relays  $L$  on the ASEP Performance**

Figure 5 presents the effect of the number of mobile relays  $L$  on the ASEP performance with QPSK modulation. The number of cascaded components is  $N=2$ . The fading coefficient is  $m=2$ . The power-allocation parameter is  $K=0.5$ . The relative geometrical gain is  $\mu=0$ dB. The given threshold is  $r_{th}=4$ dB. The number of mobile relays is  $L=1, 2, 3$ . Simulation results show that the ASEP performance is improved with the number of mobile relays  $L$  increased. For example, when  $SNR=12$ dB, the ASEP is  $3.9 \times 10^{-2}$  with  $L=1$ ,  $1.8 \times 10^{-2}$  with  $L=2$ ,  $9.5 \times 10^{-3}$  with  $L=3$ . In order to improve the ASEP performance,  $L$  should be increased. With  $L$  fixed, an increase in the SNR decreases the ASEP.



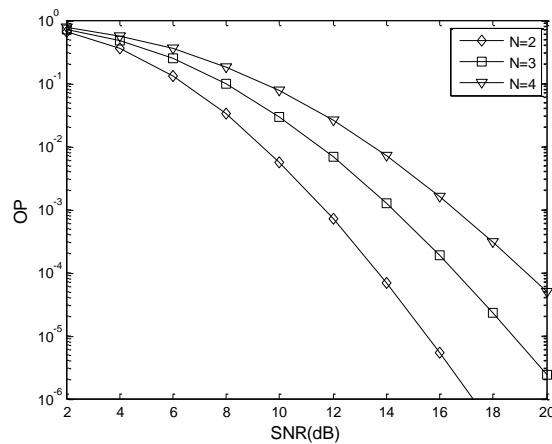
**Figure 6. The Effect of the Fading Coefficient  $M$  on the OP Performance**

Figure 6 presents the effect of the fading coefficient  $m$  on the OP performance. The number of cascaded components is  $N=2$ . The fading coefficient is  $m=1, 2, 3$ . The relative geometrical gain is  $\mu=0$ dB. The given threshold is  $r_{th}=4$ dB. The power-allocation parameter is  $K=0.5$ . The number of mobile relays is  $L=2$ . Simulation results show that the OP performance is improved with the fading coefficient  $m$  increased. For example, when  $SNR=12$ dB, the OP is  $1.2 \times 10^{-2}$  with  $m=1$ ,  $2.1 \times 10^{-2}$  with  $m=2$ ,  $4.3 \times 10^{-3}$  with  $m=3$ . This is because the fading severity of an  $N$ -Nakagami channel is reduced with a larger  $m$ . With  $m$  fixed, an increase in the SNR decreases the OP.



**Figure 7. The Effect of the Relative Geometrical Gain  $\mu$  on the OP Performance**

Figure 7 presents the effect of the relative geometrical gain  $\mu$  on the OP performance. The number of cascaded components is  $N=2$ . The fading coefficient is  $m=2$ . The relative geometrical gain is  $\mu=15$  dB, 0 dB, -15 dB. The given threshold is  $r_{th}=4$  dB. The power-allocation parameter is  $K=0.5$ . The number of mobile relays is  $L=2$ . Simulation results show that the OP performance is improved as  $\mu$  reduced. For example, when  $SNR=12$  dB, the OP is  $2.5 \times 10^{-1}$  with  $\mu=15$  dB,  $5.1 \times 10^{-3}$  with  $\mu=0$  dB, and  $1.4 \times 10^{-3}$  with  $\mu=-15$  dB. This indicates that the best location for the relay is near the destination. For a fixed  $\mu$ , an increase in the SNR reduces the OP.



**Figure 8. The Effect of the Number of Cascaded Components  $N$  on the OP Performance**

Figure 8 presents the effect of the number of cascaded components  $N$  on the OP performance. The number of cascaded components is  $N=2, 3, 4$ , which respectively denotes the 2-Nakagami, 3-Nakagami, 4-Nakagami fading channels. The fading coefficient is  $m=2$ . The relative geometrical gain is  $\mu=0$  dB. The given threshold is  $r_{th}=4$  dB. The power-allocation parameter is  $K=0.5$ . The number of mobile relays is  $L=3$ . Simulation results show that the OP performance is degraded as  $N$  increased. For example, when  $SNR=12$  dB, the OP is  $6.9 \times 10^{-4}$  with  $N=2$ ,  $6.8 \times 10^{-3}$  with  $N=3$ , and  $2.5 \times 10^{-2}$  with  $N=4$ . This is because the fading severity of the cascaded channels increases as  $N$  is increased. For fixed  $N$ , an increase in the SNR reduces the OP, as expected.

## 7. Conclusions

The exact closed-form OP expressions for the multiple-mobile-relay-based DF relaying M2M networks with relay selection over  $N$ -Nakagami fading channels are derived in this paper. The exact ASEP expressions are also presented. The simulation results show that the fading coefficient  $m$ , the number of cascaded components  $N$ , the relative geometrical gain  $\mu$ , the power-allocation parameter  $K$ , and the number of mobile relays  $L$  have an important influence on the OP and ASEP performance. The derived OP and ASEP expressions can be used to evaluate the OP and ASEP performance of the vehicular communication systems employed in inter-vehicular communications, intelligent highway applications and mobile ad-hoc applications. In the future, we will consider the impact of the correlated channels on the performance of the DF relaying M2M networks.

## Acknowledgments

The authors would like to thank the referees and editors for providing very helpful comments and suggestions. This project was supported by National Natural Science Foundation of China (No. 61304222, No. 61301139), Natural Science Foundation of Shandong Province (No.ZR2012FQ021), Shandong Province Outstanding Young Scientist Award Fund (No. 2014BSE28032), Fundamental Research Funds for the Central Universities (No. 14CX02139A).

## Appendix A

In the following subsections, we firstly evaluate  $I_1$ . According to (20), we can obtain

$$I_1 = \Pr\left(\frac{1}{2} \log_2(1 + \gamma_{SRl}) < R\right) = \Pr(\gamma_{SRl} < r_{th}) \quad (30)$$

where

$$r_{th} = 2^{2R} - 1 \quad (31)$$

With the help of [12],  $I_1$  can be given as

$$\begin{aligned} I_1 &= \int_0^{r_{th}} f_{\gamma_{SRl}}(r) dr \\ &= \frac{1}{N} \int_0^{r_{th}} \frac{1}{r} G_{0,N}^{N,0} \left[ \frac{r}{\gamma_{SRl}} \prod_{j=1}^N \frac{m_j}{\Omega_j} \middle|_{m_1, \dots, m_N}^- \right] dr \\ &= \frac{1}{N} G_{1,N+1}^{N,1} \left[ \frac{r_{th}}{\gamma_{SRl}} \prod_{j=1}^N \frac{m_j}{\Omega_j} \middle|_{m_1, \dots, m_N, 0}^1 \right] \end{aligned} \quad (32)$$

According to (4), we can obtain

$$F_{\gamma_{RDl}}(r) = \frac{1}{N} G_{1,N+1}^{N,1} \left[ \frac{r}{\gamma_{RDl}} \prod_{jj=1}^N \frac{m_{jj}}{\Omega_{jj}} \middle|_{m_1, \dots, m_N, 0}^1 \right] \quad (33)$$

where

$$\gamma_{RDl} = G_{RDl} (1 - K) \gamma \quad (34)$$

$I_2$  can be given as

$$I_2 = \left( 1 - \frac{1}{\prod_{j=1}^N \Gamma(m_j)} G_{1,N+1}^{N,1} \left[ \frac{r_{th}}{\gamma_{SRl}} \prod_{j=1}^N \frac{m_j}{\Omega_j} \Big|_{m_1, \dots, m_N, 0} \right] \right) \times \frac{1}{\prod_{jj=1}^N \Gamma(m_{jj})} G_{1,N+1}^{N,1} \left[ \frac{r}{\gamma_{RDl}} \prod_{jj=1}^N \frac{m_{jj}}{\Omega_{jj}} \Big|_{m_1, \dots, m_N, 0} \right] \quad (35)$$

## References

- [1] S. Mumtaz, K. M. S. Huq, and J. Rodriguez, "Direct mobile-to-mobile communication: Paradigm for 5G," *IEEE Wireless Communications*, vol. 21, no. 5, (2014), pp. 14-23.
- [2] M. Seyfi, S. Muhaidat, J. Liang, and M. Uysal. "Relay Selection in Dual-Hop Vehicular Networks," *IEEE Signal Processing Letters*, vol. 18, no. 2, (2011), pp. 134-137.
- [3] F.K.Gong, P.Ye, Y.Wang, N. Zhang. "Cooperative mobile-to-mobile communications over double Nakagami-m fading channels," *IET Communications*, vol. 6, no. 18, (2012), pp. 3165-3175.
- [4] G. K. Karagiannidis, N. C. Sagias, and P. T. Mathiopoulos, "N\*Nakagami: a novel stochastic model for cascaded fading channels," *IEEE Transactions on Communications*, vol. 55, no. 8, (2007), pp. 1453-1458.
- [5] E. Dahlman, S. Parkvall, and J. Skold, 4G: LTE/LTE-Advanced for Mobile Broadband. New York, NY, USA: Academic, (2011).
- [6] H. Ilhan, M. Uysal, and I. Altunbas. "Cooperative Diversity for Intervehicular Communication: Performance Analysis and Optimization," *IEEE Transactions on Vehicular Technology*, vol. 58, no.7, (2009), pp. 3301-3310.
- [7] L.W. Xu, H. Zhang, T.T. Lu, X. Liu, and Z. Q. Wei. "Performance Analysis of the Mobile-Relay-Based M2M Communication Over N-Nakagami Fading Channels," *Journal of Applied Science and Engineering*, vol. 18, no. 3, (2015), pp. 309-314.
- [8] L.W. Xu, H. Zhang, and T. A. Gulliver. "Performance Analysis of IDF Relaying M2M Cooperative Networks over N-Nakagami Fading Channels," *KSII Transactions on Internet & Information Systems*, vol. 9, no. 10, (2015), pp. 3983-4001.
- [9] H. Ochiai, P. Mitran, and V. Tarokh, "Variable-rate two-phase collaborative communication protocols for wireless networks," *IEEE Transactions on Vehicular Technology*, vol. 52, no. 9, (2006), pp. 4299-4313.
- [10] A. Papoulis. *Probability, Random Variables, and Stochastic Processes*, 3rd edition, New York: McGraw-Hill, (1991).
- [11] M. R. McKay, A. J. Grant, I. B. Collings. "Performance analysis of MIMO-MRC in double-correlated Rayleigh environments," *IEEE Transactions on Communications*, vol.55, no. 3, (2007), pp. 497-507.
- [12] A.M. Mathai and R.K. Saxena. *Generalized Hypergeometric Functions with Applications in Statistics and Physical Sciences*, New York: Springer, Heidelberg, (1973).

## Authors



**Lingwei Xu**, he was born in Gaomi, Shandong Province, China, in 1987. He received his B.E. degree in Communication Engineering from Qingdao Technological University, China in 2011. He received his M.E. degree in Electronics and Communication Engineering from Ocean University of China, China in 2013. Now he is a Ph.D. candidate in Ocean University

of China. His research interests include ultra-wideband radio systems, MIMO wireless systems, and M2M wireless communications.



**Hao Zhang**, he received his B.E. degree in Telecommunications Engineering and Industrial Management from Shanghai Jiaotong University, China in 1994. He received his MBA degree from New York Institute of Technology, USA in 2001. He received his Ph.D. degree in Electrical and Computer Engineering from the University of Victoria, Canada in 2004. From 1994 to 1997, he was the Assistant President of ICO Global Communication Company. In 2000, he joined Microsoft Canada as a Software Engineer, and was Chief Engineer at Dream Access Information Technology, Canada from 2001 to 2002. He is currently a professor in the Department of Electronic Engineering at Ocean University of China and an adjunct professor in the Department of Electrical and Computer Engineering at the University of Victoria. His research interests include ultra-wideband radio systems, MIMO wireless systems, cooperative communication networks and spectrum communications.



**T. Aaron Gulliver**, he received his Ph.D. degree in Electrical and Computer Engineering from the University of Victoria, Victoria, BC, Canada in 1989. He is a professor in the Department of Electrical and Computer Engineering. From 1989 to 1991 he was employed as a Defense Scientist at Defense Research Establishment Ottawa, Ottawa, ON, Canada. He has held academic positions at Carleton University, Ottawa, and the University of Canterbury, Christchurch, New Zealand. He joined the University of Victoria in 1999 and is a Professor in the Department of Electrical and Computer Engineering. In 2002 he became a Fellow of the Engineering Institute of Canada, and in 2012 a Fellow of the Canadian Academy of Engineering. He is also a senior member of IEEE. His research interests include information theory and communication theory, and ultra wideband communication.